International Journal of Theoretical Physics (2024) 63:37
https://doi.org/10.1007/s10773-024-05562-6

RESEARCH

The Ricci Rotation Coefficients in the Description of Trajectories of Spinning Test Particles Off-equatorial Plane in the Gravitational Field of a Rotating Source

Nelson Velandia[1] · J. Alfonso Leyva[1] · Javier Alexander Cano-Arango[1,2]

Received: 26 October 2023 / Accepted: 21 January 2024 / Published online: 6 February 2024

Abstract
We describe the trajectories of circular orbits of spinless and spinning test particles around a rotating body in equatorial and non-equatorial planes via the Mathisson-Papapetrou-Dixon equations. In this paper, these equations include the Ricci rotation coefficients with the purpose of describing not only the curvature of space time, but also the rotation of the spinning test particles that orbit around a rotating massive body. We found a numerical difference between the trajectories of spinless test particles and spinning test particles in the order of $\mathbf{10^{-7}}$. We take as parameters: radius, energy, Carter's constant and angular momentum.

Keywords Kerr metric · Mathisson-Papapetrou-Dixon equations · Carter's equations · Ricci rotation coefficients

1 Introduction

One of the ways to study the physics of a rotational gravitational field, is to describe the motion of test particles in this field. Typically in the literature, we find two main approaches to the description of the motion of spinning test particles in a rotating gravitational field in non-equatorial plane. The first one is given by Mathisson-Papapetrou-Dixon Equations (MPD) [1–3] which yields the equations of motion of a spinning test particle in a given gravitational field. The second takes the first integrals of motion given by Carter [4] and derives the orbits

✉ Nelson Velandia
navelandia@javeriana.edu.co

J. Alfonso Leyva
leyvaa@javeriana.edu.co

Javier Alexander Cano-Arango
javier.cano@correo.nucleares.unam.mx

[1] Departamento de Física, Facultad de Ciencias, Pontificia Universidad Javeriana, Cr. 7 No 40 - 62, Bogotá D.C. 110231, Colombia

[2] Departamento de Física de Altas Energías, Instituto de Ciencias Nucleares, Universidad Nacional Autónoma de México, Apartado Postal 70-543, Ciudad de México 110231, México

of spinless test particles around a rotating massive body. The term "particle" is because the size of the test body is small compared to the scale of the curvature.

The motion of particles in the Kerr type metric has been discussed by many authors [5–10]. Many of these works study the motion in the equatorial plane for spinless and spinning test particles via MPD Equations [11, 12]. Using this last formalism, we calculate the trajectories of spinless and spinning test particles in non-equatorial planes. On the other hand, in the literature, there are studies that use the Carter's equations for both spinless and spinning test particles in equatorial planes [13, 14], but there are few works that describe the motion of spinless test particles around rotating bodies in non-equatorial planes [15, 16]. This is the first novelty in relation to previous works. The majority of papers take the polar angle as $\theta = \pi/2$. In these cases, they reduce the problem only in the equatorial plane while the particles could travel around the massive body. Of course, in the numerical calculation, taking another integration variable is harder, as is the case of this angle. On the other hand, the study of trajectories of spinning test particles in non-equatorial planes for a Kerr spacetime under the Carter's equations needs further investigation. We focus our work in the formalism given by the MPD equations [2]. In this method, we are given a distribution of mass (m) with spin tensor ($S^{\rho\sigma}$) around on central source (M) which has a metric tensor $g_{\mu\nu}$. These equations of motion for a spinning test particle are obtained in terms of an expansion that depends on the derivatives of the metric and the multipole moments of the energy-momentum tensor ($T^{\mu\nu}$) [2], and are given by

$$\frac{D}{d\tau}p^{\mu}(\tau) = -\frac{1}{2}R^{\mu}{}_{\nu\rho\sigma}v^{\nu}(\tau)S^{\rho\sigma}(\tau) \tag{1}$$

$$\frac{D}{d\tau}S^{\mu\nu}(\tau) = 2p^{[\mu}(\tau)v^{\nu]}(\tau), \tag{2}$$

where $D/d\tau$ means the covariant derivative, the vector p^{μ} and the antisymmetric tensor $S^{\mu\beta}$ are the linear and spin angular momenta respectively. $R^{\mu}{}_{\nu\rho\sigma}$ is the curvature tensor [17]. Since $p_{\mu}p^{\mu} =$ constant and $S_{\rho\sigma}S^{\rho\sigma} =$ constant along the particle trajectory [18]; then, we may set

$$p^{\mu} = mu^{\mu}, \qquad u_{\mu}u^{\mu} = -1 \tag{3}$$

$$S^{\rho\sigma} = \epsilon^{\rho\sigma}{}_{\mu\nu}p^{\mu}S^{\nu} \tag{4}$$

$$S^2 = S_{\mu}S^{\mu} = \frac{1}{2m^2}S_{\mu\nu}S^{\mu\nu}, \tag{5}$$

and with these expressions, we obtain the center of mass condition and the relation between the spin tensor and the vector spin which is called spin supplementary condition (SSC). For this case, we used the Tulczyjew supplementary condition [19]:

$$p_{\mu}S^{\mu} = 0. \tag{6}$$

In the present paper, we calculate numerically, via MPD equations, the trajectories for spinless and spinning test particles in circular orbits when the test particles are in non-equatorial planes. We are interested in studying the effects from spin of the test particle orbiting in a rotating gravitational field which is generated by a massive rotating body. In the majority of cases, the description of trajectories is given by the study of the Christoffel symbols. The novelty of our work is to take the Ricci Rotation Coefficients (RRC) in order to study the trajectories of spinning test particles in non-equatorial planes. One of the properties of these coefficients is the coordinates of the derivative vectors measure not only the deviation, but also the rotation of all the frame vectors. On the other hand, when we study these trajectories,

we can describe the behavior of particles with spin in a Kerr metric and the relationship between the angular momentum of the central mass with the spin of the test particle.

The Carter's equations are given by the first integrals of the equations of motion of a spinless test particle around a rotating body for a Kerr metric both in an equatorial plane and in non-equatorial planes [4]. These equations use the symmetries of the Kerr geometry and the conserved quantities of energy (E), angular momentum (L), rest mass (M) and a fourth integral of motion called Carter's constant (Q). For the case of spinning test particles in the equatorial plane, when the space-time possesses a Killing field, there exists a linear combination of the components of momenta (p^{μ}) and the spin tensor ($S^{\mu\nu}$) [20]. The study for orbits of spinning test particles off the equatorial plane by the Carter's equations needs further investigation.

We will compare the results by numerical integration in three cases: first, we compare between trajectories of spinless test particles in a non-equatorial plane. To describe these trajectories, Carter's equations are used. In this system of equations, a conserved quantity associated with movement in the latitudinal direction is introduced. This quantity is called Carter's constant. We will compare the result of this system of equations with the trajectories given by the integration of the MPD equations that include the Ricci Rotation Coefficients (RRC). These last equations describe the motion for test particles with spin. That is, in addition to the four velocity of the particle, the components of the four spin vector are integrated. In the second case, we numerically compare the trajectories of the test particles in the system given by the MPD equations for two situations: first we integrate the MPD equations when the magnitude of the four spin vector is equal to zero and we compare when its magnitude is different from zero. This will allow us to describe the deviation of the trajectory if it has spin or if it does not. Third case, we compare the behavior of two Boyer Linquist coordinates (θ, φ) in regard to the proper time (τ) both to spinless and to spinning test particles.

The paper is organized as follows. In Section 2, the equations of motion MPD are reduced to expressions that include the Ricci Rotation Coefficients (RRC). These equations describe the motion of spinless and spinning test particles around a rotating body. We study the cases when the spinless and spinning test particles are in the equatorial plane and give the set of equations when the spinless and spinning test particles are out of the equatorial plane. In Section 3, there is a brief description of Carter's equations for spherical orbits. These equations take three constants of motion given by the symmetries of a rotating body. A fourth constant is obtained from the separability of the Hamilton-Jacobi equation. These orbits are calculated numerically. Then, in Section 4, we present a numerical comparison between the MPD equations and Carter's equations for the spinless test particles both in the equatorial plane and a non-equatorial plane. We take the initial values from Carter's equations and replace them in the MPD equations. In the last section, the conclusions and some future projects are formulated in order to describe spinning test particles in a Kerr type metric.

2 MPD Equations and the Ricci Rotation Coefficients

Generally when we solve a problem in General Relativity, we consider the field equations in a local coordinate basis. Although we can choose the basis in order to describe the physical system, this new set of equations of independent vector fields is called *tetrad*. This formalism simplifies the principal quantities of the problem. The mathematical objects are projected in the new basis for studying the problem, and then we can go back to the original basis with another projection [21].

The MPD equations had been traditionally used in the equatorial plane. We focus our study not only in the equatorial plane, but also in a non-equatorial plane. In this paper, we take the work from Tanaka et al. [11] who reduce the equations of motion using the RRC. They solve the equations of motion for a circular orbit in the equatorial plane while we, with the same method, solve the case for trajectories in a non-equatorial plane. Given this, the equations of motion (1) and (2) for the tetrad components are reduced to

$$\frac{du^\alpha}{d\tau} = \omega_{\beta\gamma}{}^\alpha v^\beta u^\gamma - SR^\alpha, \tag{7}$$

$$\frac{d\zeta^\alpha}{d\tau} = \omega_{\beta\gamma}{}^\alpha v^\beta \zeta^\gamma - Su^\alpha \zeta^\beta R_\beta. \tag{8}$$

$$v^\mu - u^\mu = \frac{1}{2}\left(\frac{S^{\mu\nu}R_{\nu\rho\sigma\kappa}u^\rho S^{\sigma\kappa}}{m^2 + \frac{1}{4}R_{\chi\xi\zeta\eta}S^{\chi\xi}S^{\zeta\eta}}\right), \tag{9}$$

where $\omega_{\beta\gamma}{}^\alpha$ are the RRC and ζ^α is the unit spin vector, which is defined by $\zeta^\alpha := S^a/S$. Here R^α and $S^{\mu\nu}$ are defined by

$$R^\alpha := R^{*\alpha}{}_{\beta\gamma\lambda}v^\beta u^\gamma \zeta^\lambda = \frac{1}{2mS}R^\alpha{}_{\beta\gamma\lambda}v^\beta S^{\gamma\lambda}. \tag{10}$$

$$S^{\gamma\lambda} := mS\epsilon^{\gamma\lambda}{}_{\vartheta\kappa}u^\vartheta \zeta^\kappa = m\epsilon^{\gamma\lambda}{}_{\vartheta\kappa}u^\vartheta S^\kappa, \tag{11}$$

the last equation yields the relation between tensor spin ($S^{\gamma\lambda}$) and the vector spin (S^κ). For our calculation, we have an orthonormal frame with the RRC and we can extract information about the curvature of the spacetime in question. It will be important when we describe the trajectories of test particles off-equatorial plane.

On the other hand, the RRC are related with the coordinates of the derivative vectors that measure not only the deviation, but also the rotation of all the frame vectors when moved in various directions [22]. Furthermore, we can observe that the RRC carry information about how the frame rotates and not just information about the curvature of spacetime.

2.1 Calculation of the Ricci Rotation Coefficients

Next, we define the Ricci rotation coefficients for a Kerr spacetime [23] as $\omega_{ab}{}^c = e_a{}^\mu e_b{}^\nu e^c{}_{\nu;\mu}$ where the semicolon indicates the covariant derivative (Appendix A).

In order to find a solution, it is convenient to introduce the tetrad frame [11] defined by $e^i{}_\mu = \left(e^i{}_t, e^i{}_r, e^i{}_\theta, e^i{}_\varphi\right)$

$$e^0{}_\mu = \left(\sqrt{\frac{r^2 - \frac{2GMr}{c^2} + a^2}{r^2 + a^2\cos^2\theta}}, 0, 0, -a\sin^2\theta\sqrt{\frac{r^2 - \frac{2GMr}{c^2} + a^2}{r^2 + a^2\cos^2\theta}}\right),$$

$$e^1{}_\mu = \left(0, \sqrt{\frac{r^2 + a^2\cos^2\theta}{r^2 - \frac{2GMr}{c^2} + a^2}}, 0, 0\right),$$

$$e^2{}_\mu = \left(0, 0, \sqrt{r^2 + a^2\cos^2\theta}, 0\right),$$

$$e^3{}_\mu = \left(-\frac{a\sin\theta}{\sqrt{r^2 + a^2\cos^2\theta}}, 0, 0, \frac{\left(r^2 + a^2\right)\sin\theta}{\sqrt{r^2 + a^2\cos^2\theta}} \right) \tag{12}$$

where the Greek letters distinguish the tensor indices ($\mu = t, r, \theta, \varphi$) from the tetrad indices which are in the Latin alphabet ($i = 0, 1, 2, 3$). Here we use the metric signature $(-, +, +, +)$.

The RRC are given by [21, 24]

$$\omega_{(a)(b)(c)} = \frac{1}{2}\left[\lambda_{(a)(b)(c)} + \lambda_{(c)(a)(b)} - \lambda_{(b)(c)(a)}\right] \tag{13}$$

where $\lambda_{(a)(b)(c)}$ are the rotation pre-coefficients and are defined by

$$\lambda_{(a)(b)(c)} = e_{(b)\mu,\nu}\left[e_{(a)}{}^\mu e_{(c)}{}^\nu - e_{(a)}{}^\nu e_{(c)}{}^\mu\right]. \tag{14}$$

In this nomenclature, the author writes the Latin letters (*a,b,c,...*) enclosed in round brackets that represent the labels of the four vectors of the tetrad, while the Greek letters (μ, ν) represent the components of the vector.

2.2 Spinless Test Particles in a Kerr Metric

In this section, the equations of motion for spinless test particles in a Kerr metric with constant radius ($r = r_0$) are solved. The aim is to write down the equations with the help of the (7) and the RRC (Appendix A). In this case, the magnitude of the spin is equal to zero ($S = 0$) and r is constant, i.e. $u^1 = 0$. Since the test particle is spinless and according to (9), it can be identified the velocity v^μ with the velocity u^μ in (7). Therefore the system of equations is given by

$$\frac{d}{d\tau}u^0 = \omega_{02}{}^0 u^0 u^2 \tag{15}$$

$$\frac{d}{d\tau}u^1 = \omega_{02}{}^1 u^0 u^2 + 2\omega_{03}{}^1 u^0 u^3 + \omega_{22}{}^1 u^2 u^2 + \omega_{33}{}^1 u^3 u^3 = 0 \tag{16}$$

$$\frac{d}{d\tau}u^2 = \omega_{00}{}^2 u^0 u^0 + 2\omega_{03}{}^2 u^0 u^3 + \omega_{33}{}^2 u^3 u^3 \tag{17}$$

$$\frac{d}{d\tau}u^3 = -2\omega_{02}{}^3 u^0 u^2 - \omega_{23}{}^3 u^2 u^3. \tag{18}$$

We replace the values of the RRC and the tetrads in (15) - (18). These latter equations for spinless test particles will be solved by numerical integration with Mathematica.

Tanaka et al. consider a class of circular orbits in the equatorial plane and assume that: $\widetilde{\theta} := \theta - \pi/2 = O(S/M) \ll 1$. In this case, r = constant ($u^1 = 0$), and close to the equatorial plane ($u^2 = O(\widetilde{\theta})$). Under this assumption, the nontrivial equation is [11]

$$\frac{d}{d\tau}u^1 = \omega_{00}{}^1 u^0 u^0 + \omega_{30}{}^1 u^3 u^0 + \omega_{03}{}^1 u^0 u^3 + \omega_{33}{}^1 u^3 u^3 = 0. \tag{19}$$

In this case, the orbital angular velocity is given by

$$\Omega = \frac{\pm\sqrt{M}}{r^{3/2} \pm \sqrt{M}a} \tag{20}$$

where M is the mass of central body and a is the angular momentum of the source.

2.3 Spinning Test Particles in a Kerr Metric

First of all, for the case of spinning test particles in circular orbits and in the equatorial plane, we assume that corresponds to: $r =$ constant ($u^1 = 0$), close to the equatorial plane ($u^2 = \widetilde{O(\theta)}$), and with the magnitude of spin ($S^2 = S_\mu S^\mu$). In this case, according to (7), the nontrivial equations of the orbital motion are [11]

$$\begin{aligned}\frac{d}{d\tau}u^1 &= \omega_{00}{}^1 u^0 u^0 + \omega_{30}{}^1 u^3 u^0 + \omega_{03}{}^1 u^0 u^3 + \omega_{33}{}^1 u^3 u^3 - SR^1 = 0\\ \frac{d}{d\tau}u^2 &= \left(\omega_{00}{}^2 u^0 u^0 + \omega_{30}{}^2 u^3 u^0 + \omega_{03}{}^2 u^0 u^3 + \omega_{33}{}^2 u^3 u^3\right)\widetilde{\theta} - SR^2\end{aligned} \tag{21}$$

where the components of R^a are given by

$$\begin{aligned}R^0 &= R^3 = \widetilde{O(\theta)}\\ R^1 &= 3\frac{M}{r^3}u^0 u^3 \frac{S^2}{S} + \widetilde{O(\theta)}\\ R^2 &= 3\frac{M}{r^3}u^0 u^3 \frac{S^1}{S} + \widetilde{O(\theta)}.\end{aligned} \tag{22}$$

In the equatorial plane, the orbital angular velocity for spinning test particles is given by

$$\Omega = \pm\frac{\sqrt{M}}{r^{3/2} \pm a\sqrt{M}}\left[1 - \frac{3S}{2}\frac{\pm\sqrt{Mr} - a}{r^2 \pm a\sqrt{Mr}}\right] + \widetilde{O(\theta)}. \tag{23}$$

This new expression corresponds to the spin contribution (S) at $\widetilde{O(\theta)}$.

Now for the non-equatorial orbits; first, we take the work by Tanaka et al. [11] which studies the motion of the spinning test particle in the equatorial plane, and then, we go one step further and numerically calculate the trajectories of off-equatorial orbits. For this treatment, we replace the "dynamical velocity v" (9) in (7) and (8), and obtain the set of equations:

$$\begin{aligned}\frac{du^\alpha}{d\tau} &= \omega_{\beta\gamma}{}^\alpha\left(u^\beta + \frac{\epsilon^{\beta\nu}{}_{\varphi\lambda}u^\varphi S^\lambda R_{\nu\rho\sigma\kappa}u^\rho \epsilon^{\sigma\kappa}{}_{\tau\upsilon}u^\tau S^\upsilon}{8 + 2R_{\chi\xi\zeta\eta}\epsilon^{\chi\xi}{}_{\iota\varphi}u^\iota S^\varphi \epsilon^{\zeta\eta}{}_{\delta\varepsilon}u^\delta S^\varepsilon}\right)u^\gamma\\ &\quad -\frac{1}{2}g^{\alpha\eta}R_{\eta\mu\rho\pi}\left(u^\mu + \frac{\epsilon^{\mu\nu}{}_{\gamma\lambda}u^\gamma S^\lambda R_{\nu\rho\sigma\kappa}u^\rho \epsilon^{\sigma\kappa}{}_{\omega\vartheta}u^\omega S^\vartheta}{8 + 2R_{\chi\xi\zeta\eta}\epsilon^{\chi\xi}{}_{\iota\varphi}u^\iota S^\varphi \epsilon^{\zeta\eta}{}_{\delta\varepsilon}u^\delta S^\varepsilon}\right)\epsilon^{\rho\pi}{}_{\sigma\kappa}u^\sigma S^\kappa\end{aligned} \tag{24}$$

$$\begin{aligned}\frac{dS^\alpha}{d\tau} &= \omega_{\beta\gamma}{}^\alpha\left(u^\beta + \frac{\epsilon^{\beta\nu}{}_{\varphi\lambda}u^\varphi S^\lambda R_{\nu\rho\sigma\kappa}u^\rho \epsilon^{\sigma\kappa}{}_{\tau\upsilon}u^\tau S^\upsilon}{8 + 2R_{\chi\xi\zeta\eta}\epsilon^{\chi\xi}{}_{\iota\varphi}u^\iota S^\varphi \epsilon^{\zeta\eta}{}_{\delta\varepsilon}u^\delta S^\varepsilon}\right)S^\gamma\\ &\quad -\frac{1}{2}u^\alpha S^\beta R_{\beta\rho\lambda\mu}\left(u^\rho + \frac{\epsilon^{\rho\nu}{}_{\varphi\lambda}u^\varphi S^\lambda R_{\nu\rho\sigma\kappa}u^\rho \epsilon^{\sigma\kappa}{}_{\tau\upsilon}u^\tau S^\upsilon}{8 + 2R_{\chi\xi\zeta\eta}\epsilon^{\chi\xi}{}_{\iota\varphi}u^\iota S^\varphi \epsilon^{\zeta\eta}{}_{\delta\varepsilon}u^\delta S^\varepsilon}\right)\epsilon^{\lambda\mu}{}_{\phi\delta}u^\phi S^\delta.\end{aligned} \tag{25}$$

For the numerical integration, we need the initial values of the four velocities which will be obtained from the Carter's equations.

3 Equations of Motion and Carter's Constant

In a Kerr type manifold, the symmetries provide three constants of motion: the energy (E), the angular momentum (L), and the rest central mass (M). In addition, there is another constant

which is due to the separability of the Hamilton - Jacobi equation and is called Carter's constant (Q). The equation of Lagrange for a Kerr metric leads immediately to the first integrals of the t and φ equations, and the other two integrals of (r) and (θ) are obtained by a separable solution of the Hamilton - Jacobi equation. The set of equations is given by [25]

$$\Sigma \dot{t} = a\left(L - aE\sin^2\theta\right) + \frac{r^2+a^2}{\Delta}\left[E\left(r^2+a^2-aL\right)\right], \tag{26}$$

$$\Sigma \dot{r}^2 = \left[E\left(r^2+a^2\right) \mp aL\right]^2 - \Delta\left[r^2 + Q + (L \mp aE)^2\right], \tag{27}$$

$$\Sigma \dot{\theta}^2 = Q - \cos^2\theta\left[a^2\left(1-E^2\right) + \frac{L^2}{\sin^2\theta}\right], \tag{28}$$

$$\Sigma \dot{\varphi} = \frac{L}{\sin^2\theta} - aE + \frac{a}{\Delta}\left[E\left(r^2+a^2\right) - aL\right], \tag{29}$$

where L, E, and Q are constants and

$$\Sigma := r^2 + a^2\cos^2\theta,$$
$$\Delta := r^2 + a^2 - 2Mr,$$

M, and $a = J/Mc$ denote the central mass and specific angular momentum of the central source which gives rise to the gravitational field represented by the Kerr space-time.

In the study of orbits of test particles around on Kerr metric, there exists a kind of orbits called spherical, i.e., constant radius. This last orbit intersects the equatorial plane in a point called a node. Since the metric has angular momentum, the nodes of spherical orbits are dragged in the sense of the spin of the rotating body. When there is a particle orbiting in a nonequatorial orbit, this traces a kind of helix until a maximum of latitude, and when it reaches the maximum this begins to descend until a minimum latitude which is symmetric to the maximum [26].

When the space-time admits a Killing vector ξ^ν, there exists a property that includes the covariant derivative and the spin tensor, which gives a constant and is given by the expression [20]

$$p^\nu \xi_\nu + \frac{1}{2}\xi_{\nu,\mu} S^{\nu\mu} = \text{ constant}, \tag{30}$$

where p^ν is the linear momentum, $\xi_{\nu,\mu}$ is the covariant derivative of the Killing vector, and $S^{\nu\mu}$ is the spin tensor of the particle. In the case of a Kerr metric, there are two Killing vectors, owing to its stationary and axisymmetric nature. As consequence, (30) yields two constants of motion: E is the total energy and L is the component of its angular momentum along the axis of symmetry. Unfortunately, there is not a constant of motion associated to the coordinate r; therefore, for this method, there does not exist a equation of motion that connects the constant of motion linked to coordinate r and the spin tensor. This mathematical expression needs further investigation.

On the other hand, people avoid the error that shows the numerical integration due to the explicit square roots in the r and θ in (27) and (28). In this formulation, they take the Hamilton's canonical equations which denote differentiation of the Hamiltonian with respect to r and θ. This demonstration is based on a taxonomy of all periodic orbits around black holes [27]. The set of equations constitutes a smooth system of ordinary differential equations and can be integrated without change of variables. These equations were integrated numerically to generate the periodic orbits. These orbits describe the motion of test particles out of equatorial plane, but this approach does not take into account the spinning test particles. So far, there is not a work that connects successfully the equations of motion given by Carter and spin of

the test particle. Within Carter's equations, one finds in the literature a number of works, but none considers the spinning test particle out of the equatorial plane [28].

4 Numerical Integration of the Equations of Motion

In this section of this paper, we study the MPD Equation not so much with the Christoffel symbols, but with the RRC, which describe the trajectories of spinning test particles around rotating massive bodies. Now, we shall compare numerically the trajectories of the test particles, both the spinless and spinning. For this comparison, first we need to compare the trajectories of the spinless test particles given by the Carter's equations with the trajectories given by MPD equations. In this case, we take as parameters: radius constant $r = 10$, $E = 0.9525$, $a = 1$, $Q = 4.224806$, $L = 2.810974$, maximum latitude = 53.92928° and magnitude of spin equal to zero. We replace these values in the Equations of Carter (26) - (29) and find the initial values of the four velocities: $dt_0/d\tau = 1.00748$, $d\theta_0/d\tau = 2.854 \times 10^{-3}$, and $d\varphi_0/d\tau = 8.255 \times 10^{-1}$. Then, these initial values of the four velocities are replaced in the set of MPD equations for spinless test particles (15), (17) and (18). We plot in 3D the trajectory for a spinless test particle in Mathematica (Fig. 1). Finally, we compare the data table of the Cartesian coordinates both the Carter's equations and MPD equations, and find that the difference of values is in the order of 10^{-7}.

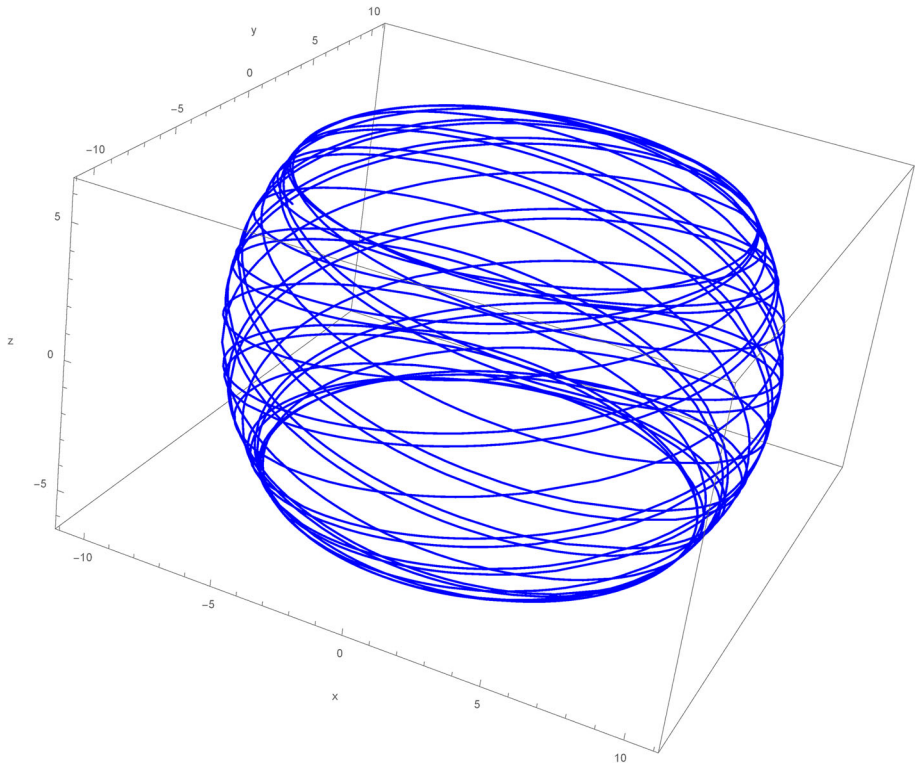

Fig. 1 Trajectory for a spinless test particle (blue color). The values of the parameters are: $r = 10$, $M = 1$, $E = 0.9525$, $a = 1$, $Q = 4.224806$, $L = 2.810974$

Next step, we compare the trajectory of a spinless test particle (15), (17), (18), with the trajectory of a spinning test particle (24), (25) in non-equatorial planes via MPD equations. The components of the four vector of spin are: $s_0 = s_t = 4.2 \times 10^{-4}, s_1 = s_r = 1.23 \times 10^{-5}$, $s_2 = s_\theta = 9.9 \times 10^{-5}, s_3 = s_\phi = 1.99 \times 10^{-4}$. We replace the values of the RRC and the non vanishing components of the curvature tensor given by Mino [23]. Then, we plot in 3D the trajectories both for a spinless test particle and a spinning test particle in Mathematica (Fig. 2). And finally, we compare the data table of the cartesian coordinates both for a spinless test particle and a spinning test particle, and find that the difference of values is in the order of 10^{-4}. This small difference in the trajectories is given by the effect of spin in a test particle [29].

We make another numerical comparison of our results given by the MPD equations in regard to the trajectories of spinless and spinning test particles. In this case, we take the same initial values for the four velocities given above which were obtained by the Carter's equations (26) - (29), and replace these initial values in the MPD equations (24), (25). Then, we take two Boyer Lindquist coordinates (θ, φ) and obtain a graph for each coordinate in regard to the proper time (τ) which show the difference in the trajectories between the spinless and spinning test particles. The first one is the figure of the polar angle versus proper time (θ vs τ) (Fig. 3). In this graph, we find the period of the spinning test particle is longer than the period of the spinless test particle. Moreover, in each orbit, the difference between the

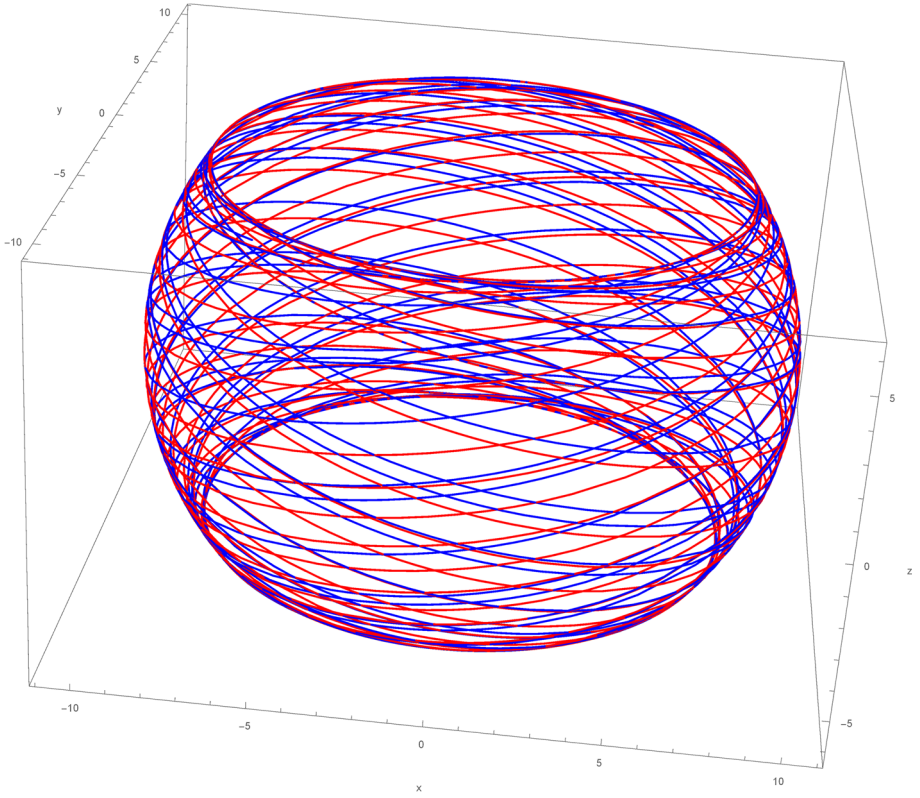

Fig. 2 Trajectories for spinless (blue color) and spinning test particles (red color). The values of the parameters are: $r = 10, M = 1, E = 0.9525, a = 1, Q = 4.224806, L = 2.810974, s_0 = 4.2 \times 10^{-4}, s_1 = 1.23 \times 10^{-5}$, $s_2 = 9.9 \times 10^{-5}, s_3 = 1.99 \times 10^{-4}$

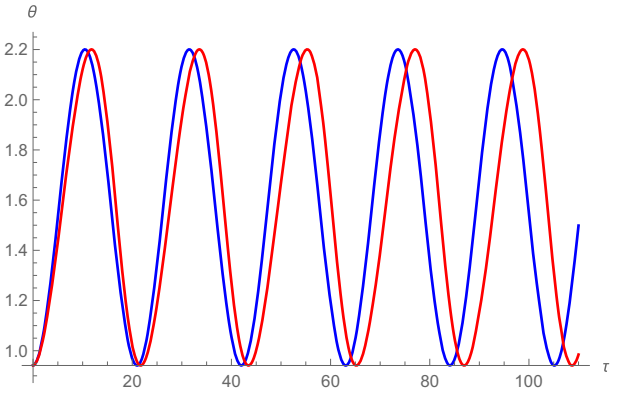

Fig. 3 Graph of polar angle (θ) vs proper time (τ) for spinless (blue color) and spinning test particles (red color). The initial conditions are: $\theta_0 = 0.9412$, $d\theta_0/d\tau = 0.03253$, $L = 2.810974$, $s_0 = 4.2 \times 10^{-4}$, $s_1 = 1.23 \times 10^{-5}$, $s_2 = 9.9 \times 10^{-5}$, $s_3 = 1.99 \times 10^{-4}$

trajectories of each test particle increases, that is, it is an accumulative process. This is due to the contribution of the value of spin in the trajectory. The test particle starts in the polar initial angle ($\theta_0 = 53.92928°$) and reaches the maximum value in the opposite side of the equatorial plane ($\theta_{op} = 143.2928°$). One can see in this graph that both the spinless and spinning test particles reach the same maximum and minimum of latitude, but with a time difference for the two paths. This is due to the precession of the spinning test particle.

As we wrote above, the difference in values between particles without spin and those with spin is the order of 10^{-4}. This difference is significant when we compare it with the error of the numerical method, which is the order of 10^{-8}. In the other words, the fact that the particle has spin brings as a consequence that it separates from the trajectory of the geodesic. This graph (Fig. 3), which is in natural units, shows the difference for each period and the increase in the difference when it advances in proper time.

The second figure shows the relation between the azimuthal angle and the proper time (Fig. 4). We find the slope of the graph for the spinning test particle is winding with relation to the graph of the spinless particle. This phenomenon is another effect of the spin of the

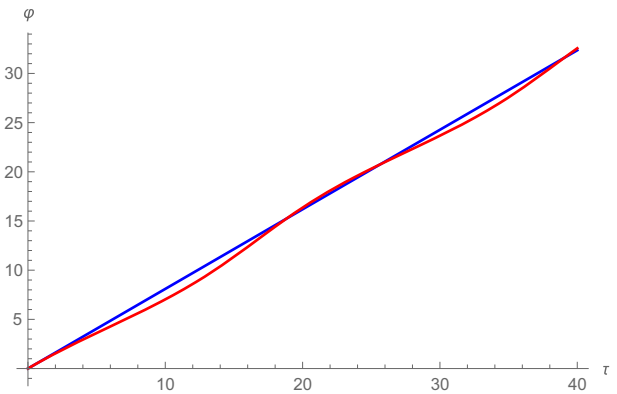

Fig. 4 Graph of azimuthal angle (φ) vs proper time (τ) for spinless (blue color) and spinning test particles (red color). The initial conditions are: $\varphi_0 = 0$, $d\varphi_0/d\tau = 0.08255$, $L = 2.810974$, $s_0 = 4.2 \times 10^{-4}$, $s_1 = 1.23 \times 10^{-5}$, $s_2 = 9.9 \times 10^{-5}$, $s_3 = 1.99 \times 10^{-4}$

particle [30] and like the previous graph this winding is due to the nutation of the spinning particle. The MPD equations described with the help of the RRC allow characterizing these phenomena.

5 Conclusions

We found that the equations of motion for spinning test particles in the MPD equations (7) - (9) describe the relation between the spin of the particle and the angular momentum of the central mass. For this case, we take the variation of spin vector in the time and the first term includes as much from the density of angular momentum (a) as from the spin of the test particle (S). For the case of spin - orbit perturbation, the equations yield the relation between the spin of the particle given by the magnitude of spin (S) and the orbit given to both the curvature tensor ($R^{\alpha}{}_{\beta\gamma\lambda}$) and the velocity of center of mass (v^{μ}).

For circular orbits close to equatorial plane, the difference of trajectories between spinless test particles and spininng test particles is very small; but when the particles have spin the difference in the time is bigger than when the particles does not have it.

The majority of works that include the Christoffel symbols in the MPD equations give a description of the coupling between spin and field while in this paper, since we include the RRC in the MPD equations, we study not only this coupling, but also the rotation of the frame that travels with the test particle. Both the Christoffel symbols and Ricci coefficients are two mathematical tools that describe the geometry of curved spacetime and study of trajectories of spinning test particles in the presence of matter and energy.

Additionally the results obtained in this paper may be important guidelines when studying accretion disks around rotating massive bodies. Since the particles around the central mass orbit above the equatorial plane, it is possible to study in general what happens inside of this accretion disk.

Appendix A: The Ricci Rotation Coefficients of the Kerr Spacetime

The non vanishing components are

$$\omega_{01}{}^{0} = \omega_{00}{}^{0} = \omega_1, \quad \omega_1 := \frac{1}{\Sigma^{3/2}\Delta^{\frac{1}{2}}}\left(ra^2\sin^2\theta - Mr^2 + Ma^2\cos^2\theta\right), \tag{A1}$$

$$\omega_{31}{}^{0} = \omega_{30}{}^{1} = \omega_{13}{}^{0} = \omega_{10}{}^{3} = \omega_{03}{}^{1} = -\omega_{01}{}^{3} = \omega_2, \quad \omega_2 := \frac{ar\sin\theta}{\Sigma^{3/2}}, \tag{A2}$$

$$\omega_{22}{}^{1} = -\omega_{21}{}^{2} = \omega_{33}{}^{1} = -\omega_{31}{}^{3} = \omega_3, \quad \omega_3 := \frac{r\Delta^{\frac{1}{2}}}{\Sigma^{3/2}}, \tag{A3}$$

$$\omega_{02}{}^{0} = \omega_{00}{}^{2} = \omega_{12}{}^{1} = -\omega_{11}{}^{2} = \omega_4, \quad \omega_4 := \frac{a^2\cos\theta\sin\theta}{\Sigma^{3/2}} \tag{A4}$$

$$\omega_{32}{}^{0} = \omega_{30}{}^{2} = -\omega_{23}{}^{0} = -\omega_{20}{}^{3} = \omega_{03}{}^{2} = -\omega_{02}{}^{3} = \omega_5, \quad \omega_5 := \frac{a\cos\theta\Delta^{\frac{1}{2}}}{\Sigma^{3/2}} \tag{A5}$$

$$\omega_{33}{}^{2} = -\omega_{32}{}^{3} = \omega_6, \quad \omega_6 := \frac{\left(r^2+a^2\right)\cos\theta}{\Sigma^{3/2}\sin\theta}. \tag{A6}$$

Here we follow the notation $\omega_1 - \omega_6$ [11] and group the components of same value with a simple index ω_i $(i = 1 - 6)$. Where: a is the angular momentum of the source, $\Sigma := r^2 + a^2 \cos^2\theta$ and $\Delta := r^2 + a^2 - 2Mr$.

Acknowledgements The authors are grateful with Pontificia Universidad Javeriana at Bogotá. The computations were performed at the Computational Centers of the Pontificia Universidad Javeriana.

Funding Open Access funding provided by Colombia Consortium. This study was funded by by the Vicerrectoria de Investigación of Pontificia Universidad Javeriana under grant number 08947.

Data Availibility The data that support the findings of this study are available from the corresponding author upon reasonable request.

Code Availability The code associated with this study is available from the corresponding author upon reasonable request.

Declarations

Ethics approval This article does not contain any studies with animals performed by any of the authors.

Consent to participate Not applicable.

Consent for publication Not applicable.

Conflict of interest The authors declare no competing interests.

References

1. Corinaldesi, E., Papapetrou, A.: Spinning test particles in general relativity ii. Proc. Roy. Soc. Lond. A. **209**(1097), 259–268 (1951)
2. Dixon, W.G.: Dynamics of extended bodies in general relativity iii equations of motion. Phil. Trans. Roy. Soc. Lond. A. **277**(1264), 59–119 (1974)
3. Mathisson, M.: Republication of: New mechanics of material systems. Gen. Rel. Grav. **42**(4), 985–987 (2010). https://doi.org/10.1007/s10714-010-0938-z
4. Carter, B.: Global structure of the kerr family of gravitatonal fields. Phys. Rev. **174**(5), 1559–1571 (1968)
5. Bardeen, J., Press, W., Teukolsky, A.: Rotating black holes: Locally nonrotating frames, energy extraction, and scalar synchrotron radiation. Astrophy. J. **178**, 347–370 (1972)
6. Dadhich, N., Kale, P.P.: Equatorial circular geodesics in the kerr-newman. J. Math. Phys. **18**(9), 1727–1728 (1977)
7. Bini, D., Geralico, A., Jantzen, R.: Kerr metric, static observers and fermi coordinate. Class. Quantum Grav. **22**(22), 4729–4742 (2005). https://doi.org/10.1088/0264-9381/22/22/006
8. Tartaglia, A.: Geometric treatment of the gravitomagnetic clock effect. Gen. Rel. Grav. **32**(9), 1745–1756 (2000). https://doi.org/10.1023/A:1001998505329
9. Plyatsko, R., Stefanyshyn, O., Fenyk, M.: Highly relativistic spinning particle starting near $r_{ph}^{(-)}$ in a Kerr field. Phys. Rev D. **82**, 044015–10 (2010). https://doi.org/10.1103/PhysRevD.82.044015

10. Plyatsko, R., Fenyk, M.: Highly relativistic circular orbits of spinning particle in the Kerr field. Phys. Rev D. **87**, 044019 (2013). https://doi.org/10.1103/PhysRevD.87.044019
11. Tanaka, T., Mino, Y., Sasaki, M., Shibata, M.: Gravitational waves from a spinning particle in circular orbits around a rotating black hole. Phys. Rev. D. **54**(6), 3762–3777 (1996). https://doi.org/10.1103/PhysRevD.54.3762
12. Suzuki, S., Maeda, K.: Innermost stable circular orbits of a spinning particle in kerr spacetime. Phys. Rev. D. **58**(2), 023005–1 (1998). https://doi.org/10.1103/PhysRevD.58.023005
13. Abramowicz, M., Calvani, M.: Spinning particles orbiting the kerr black hole. Mon. Not. R. Astron. Soc. **189**(3), 621–626 (1979). https://doi.org/10.1093/mnras/189.3.621
14. Tod, K.P., De Felice, F., Calvani, M.: Spinning test particles in the field of a black hole. Il Nouvo Cimento. **34B**(2), 365–379 (1976)
15. Wilkins, D.: Bound geodesics in the kerr metric. Phys. Rev. D. **5**(4), 814 (1972). https://doi.org/10.1103/PhysRevD.5.814
16. Tsoubelis, D., Economou, A., Stoghianidis, E.: Local and global gravitomagnetic effects in kerr spacetime. Phys. Rev. D. **36**(4), 1045–1052 (1987). https://doi.org/10.1103/PhysRevD.36.1045
17. Mohseni, M.: Lagrangian description of world-line deviations. Int. J. Theor. Phys. **47**(4), 1079–1082 (2008). https://doi.org/10.1007/s10773-007-9535-7
18. Wald, R.: Gravitational spin interaction. Phys. Rev. D. **6**(2), 406–413 (1972). https://doi.org/10.1103/PhysRevD.6.406
19. Kyrian, K., Semerák, O.: Spinning test particles in a kerr field - ii. Mon. Not. R. Astron. Soc. **382**(4), 1922–1932 (2007). https://doi.org/10.1111/j.1365-2966.2007.12502.x
20. Ehlers, J. (ed.): Isolated Gravitating Systems in General Relativity. North-Holland, Amsterdam (1979)
21. Larrañaga, A.: Black Holes I Geometric Description. https://arxiv.org/ (2013)
22. Gogala, B.: Torsion and related concepts: An introductory overview. Int. J. Theor. Phys. **19**(8), 573–586 (1980). https://doi.org/10.1007/BF00669602
23. Mino, Y., Shibata, M., Tanaka, T.: Gravitational waves induced by a spinning particle falling into a rotating black hole. Phys. Rev. D. **53**(2), 622–634 (1996). https://doi.org/10.1103/PhysRevD.53.622
24. Chandrasekhar, S.: The Mathematical Theory of Black Holes. Oxford University Press, Oxford (1983)
25. Stoghianidis, E., Tsolubelis, D.: Polar orbits in the kerr space-time. Gen. Rel. and Grav. **19**(12), 1235–1249 (1987). https://doi.org/10.1007/BF00759103
26. Kheng, L., Perng, S., Sze Jackson, T.: Massive Particle Orbits Around Kerr Black Hole. Paper presented at the National University of Singapore Semester I (2007)
27. Levin, J., Perez-Giz, G.: A periodic table for black hole orbits. Phys. Rev. D. **77**(10), 103005 (2008). https://doi.org/10.1103/PhysRevD.77.103005
28. Iorio, L.: General relativistic spin-orbit and spin-spin effects on the motion of rotating particles in an external gravitational field. Gen. Rel. and Grav. **44**(3), 719–736 (2012). https://doi.org/10.1007/s10714-011-1302-7
29. Mashhoon, B., Singh, D.: Dynamics of extended spinning masses in a gravitational field. Phys. Rev. D. **74**(12), 124006 (2006). https://doi.org/10.1103/PhysRevD.74.124006
30. Mashhoon, F.B., Hehl, F.W., Theiss, D.: On the gravitational effects of rotating masses: The thirring-lense papers. Gen. Rel. and Grav. **16**(8), 711–750 (1984). https://doi.org/10.1007/BF00762913